THE JOURNAL OF PHYSICAL CHEMISTRY LETTERS
A JOURNAL OF THE AMERICAN CHEMICAL SOCIETY

pubs.acs.org/JPCL

Letter

Mean Value Ensemble Hubbard-*U* Correction for Spin-Crossover Molecules

Angel Albavera-Mata, S. B. Trickey,* and Richard G. Hennig*

Cite This: *J. Phys. Chem. Lett.* 2022, 13, 12049−12054

Read Online

ACCESS | Metrics & More | Article Recommendations | Supporting Information

ABSTRACT: High-throughput searches for spin-crossover molecules require Hubbard-*U* corrections to common density functional exchange-correlation (XC) approximations. However, the U_{eff} values obtained from linear response or based on previous studies overcorrect the spin-crossover energies. We demonstrate that employing a linearly mixed ensemble average spin state as the reference configuration for the linear response calculation of U_{eff} resolves this issue. Validation on a commonly used set of spin-crossover complexes shows that these ensemble U_{eff} values consistently are smaller than those calculated directly on a pure spin state, irrespective of whether that be low- or high-spin. Adiabatic crossover energies using this methodology for a generalized gradient approximation XC functional are closer to the expected target energy range than with conventional U_{eff} values. Based on the observation that the U_{eff} correction is similar for different complexes that share transition metals with the same oxidation state, we devise a set of recommended averaged U_{eff} values for high-throughput calculations.

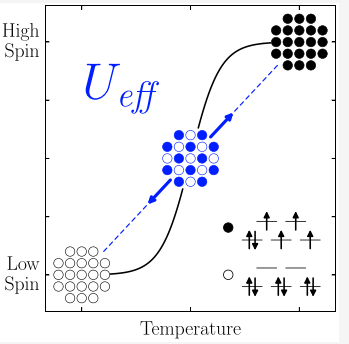

The interactions between transition metal ions with surrounding homoleptic or heteroleptic ligands result in a splitting of the *d*-manifold that favors a low-spin (LS) state if the metal−ligand interaction is strong or a high-spin (HS) state if it is weak.[1] For intermediate strength interactions, reversible switching between the two spin-states can be possible[2] if the interactions are responsive to an external perturbation such as temperature or pressure change, light pulse, or applied magnetic field. Such switching is known as spin-crossover (SCO). Example systems include metal−organic complexes that switch not only the spin-state but also their electronic state and coordination structure. Those concurrent changes make such molecules particularly attractive for electronic devices in memory, display, and sensing applications.[3,4] Therefore, an obvious goal for theoretical and computational materials studies is to search and screen for promising SCO candidate molecules and their aggregates.[5−9]

For such a search of SCO materials, the dominance of predictive calculations of molecular and condensed phase properties based on density functional theory (DFT) weighs in favor of using it. Relatively simple exchange-correlation (XC) density functional approximations (DFAs) are important in this context because the size and complexity of bistable molecular complexes pose a computational cost challenge. For example, adiabatic crossover energy differences have been matched with good accuracy by using hybrid DFAs that include an explicit single-determinant exchange contribution.[10−14] However, the relatively high computational cost of hybrid DFAs and the sensitivity of their predictions to the hybridization fraction[13,15,16] constitute a significant barrier to computational large-scale screening and exploration. Therefore, the use of generalized gradient approximation (GGA) or meta-GGA density functionals remains important.

It is well-known, however, that the proper theoretical description of the *d*-manifold for the molecules of interest poses a problem for such currently available cost-effective DFAs. The difficulty is that they have spurious self-interaction and fail to have proper derivative discontinuities in the total energy.[17−19] Those issues arise either with respect to the total number of electrons defined in a special grand ensemble or with respect to the total spin—but not particle number—in the same kind of special grand ensemble.[20,21]

Several approximate prescriptions have been proposed to counteract the self-interaction and to handle the static correlation that underlies its severity.[22−25] For strong correlation, the Hubbard model often is used as a computationally efficient alternative to describe the localized *d*-orbital population. The magnitude of the Hubbard-*U* parameter is considered to be a linear response property of the transition-metal *d*-electrons,[26] whereas the remaining valence electrons are treated with a conventional DFA.[27] The combination is known as DFA+*U*. The caveat, however, is that the Hubbard-*U* magnitude lacks a unique definition; hence, different determination methods yield different *U* values.[28−32]

Received: November 7, 2022
Accepted: December 9, 2022

https://doi.org/10.1021/acs.jpclett.2c03388
J. Phys. Chem. Lett. 2022, 13, 12049−12054

An appealing feature of DFA+U for the description of the molecular bistability characteristic of spin crossover transitions is the partial restoration of proper piecewise linear behavior of the total energy with respect to the on-site orbital occupation. The Hubbard correction introduces a discontinuity in the potential that acts on the localized d-states. That, in turn, compensates for part of the missing derivative discontinuity in the approximate XC potential.[33,34] For localized states that correspond to the frontier orbitals from the valence and conduction manifolds, an adequate Hubbard-U value improves the description of the electronic state for an otherwise omitted or inadequate treatment of correlated electrons.[35]

The partial corrective effect of using the Hubbard-U resembles that of single-determinant exchange in hybrid DFAs,[36,37] although they are not designed for strong correlation. In crossover transitions, both approaches are known to stabilize the HS relative to the LS state as their contributions increase.[13,15,16,38−41] However, that signals another problem. The large Hubbard-U values that often are the result of a conventional linear-response method can lead to inconsistent crossover descriptions.[40,42−45] Note, for example, the approach taken in ref 45, an empirical fitting of a single U independent of the LS or HS state. The remark at the end of Section 2.4 of that reference states that the "...method does not seem suitable to describe the spin-state energetics of SCO compounds..." because "...the resulting U values are, thus, overestimated...". Essentially, the problem is one of over-correction that is problematic for high-throughput screening.[46]

In what follows, we avoid fitting U values to match experimental data and instead address these issues by determining a single nonempirical U_{eff} from an ensemble average between the configurations of both spin-states that serves as a realistic reference state. Results for a set of bistable species show that crossover energies improve with this methodology when it is used with an orbital-independent, hence low-cost, DFA. We also observe that the calculated correction is similar for different complexes that share transition metals with the same oxidation state. Based on that observation, we provide a set of recommended effective Hubbard-U values for a series of 3d transition metal ions for possible use in automated high-throughput methods.

We start with the definition and characteristics of the reference state to be used for the U_{eff} calculation. Consider an N-electron system with some external control parameter such that, depending upon the parameter value, there are two possible pure ground states corresponding to LS and HS populations, respectively. We label them as Ψ_{LS}, Ψ_{HS} with respective ground-state energies E_{LS}, E_{HS}, and associated ground-state electron number densities $n_{LS}(\mathbf{r})$, $n_{HS}(\mathbf{r})$.

The total energy per molecule of a linearly mixed ensemble of the two pure states, Ψ_{LS} and Ψ_{HS}, is

$$\tilde{E}_{\omega} = (1 - \omega)E_{LS} + \omega E_{HS} \tag{1}$$

and the ensemble electron number density is

$$\tilde{n}_{\omega}(\mathbf{r}) = (1 - \omega)n_{LS}(\mathbf{r}) + \omega n_{HS}(\mathbf{r}) \tag{2}$$

with $0 \leq \omega \leq 1$.[21]

Three values are of interest for describing a continuous and complete crossover from Ψ_{LS} to Ψ_{HS}, and vice versa without hysteresis, namely, the pure LS state ($\omega = 0$), the equally mixed state ($\omega = {}^1/_2$), and the pure HS ($\omega = 1$) state. Their ensemble energies read

$$\tilde{E}_{\omega=0} = E_{1/2} - \frac{1}{2}\Delta E_{HL} \tag{3}$$

$$\tilde{E}_{\omega=1/2} = E_{1/2} \tag{4}$$

$$\tilde{E}_{\omega=1} = E_{1/2} + \frac{1}{2}\Delta E_{HL} \tag{5}$$

where the average energy per molecule of the mixed state, according to eq 1, is $E_{1/2} = (E_{LS} + E_{HS})/2$ and the energy difference per molecule between the reference pure states Ψ_{LS} and Ψ_{HS} is $\Delta E_{HL} = E_{HS} - E_{LS}$. Notice that the value of ΔE_{HL} here is for the pure states associated with whatever uncorrected DFA is chosen. It is not the eventual ΔE_{HL} value calculated with the Hubbard-U.

The analogous analysis for the spins S_{LS}, S_{HS} for Ψ_{LS}, Ψ_{HS} leads to

$$\tilde{S}_{\omega=0} = S_{1/2} - \frac{1}{2}\Delta S_{HL} \tag{6}$$

$$\tilde{S}_{\omega=1/2} = S_{1/2} \tag{7}$$

$$\tilde{S}_{\omega=1} = S_{1/2} + \frac{1}{2}\Delta S_{HL} \tag{8}$$

with $S_{1/2} = (S_{LS} + S_{HS})/2$ being the average spin per molecule of the mixed state and $\Delta S_{HL} = S_{HS} - S_{LS}$ the change in spin from Ψ_{LS} to Ψ_{HS}.

As a result of the linearity of eqs 1 and 2, the mean value ensemble spin (MS) state with spin $S_{1/2}$, located at an equidistant energy separation of $\frac{1}{2}\Delta E_{HL}$ with respect to either of the pure states, may be considered as an appropriate reference state to calculate an effective Hubbard-U correction for SCO through linear response.[29] The physical motivation is that the ensemble state corresponds to the most appropriate simple representation of the bistable pure state problem.

The mean value ensemble spin-state is not unique but depends upon the choice of pure system states, for example, whether they be from isolated molecules or crystalline systems. Furthermore, unlike the fractional electron ensemble familiar since the work of Perdew, Parr, Levy, and Baldúz[20] and the Slater transition state half-electron interpolation that preceded it,[47,48] we cannot probe the mean value ensemble with a single molecule having a single transition metal for the elementary reason that there is no half-spin that corresponds to the half-electron associated with occupation number $n_i = {}^1/_2$. Thus, the MS state must comprise equal populations of LS and HS molecules.

The simplest, least computationally costly choice is one molecule of each pure state, LS and HS. The concept is roughly that of picking a local sample in a 1:1 LS:HS solution.[49,50] There remains the issue of criteria for choosing an appropriate sample configuration of the molecules. In the present case, we chose the ensemble state to be built on the assumption that the most strongly interacting sample in the condensed phase is the nearest-neighbor pair of molecules in the crystalline environment with atomic coordinates obtained from the experimental data. Figure 1 shows that the choice of atomic configuration only affects the resulting U_{eff} weakly, with deviations well within accepted magnitudes.[51] The protocol then is as follows:

https://doi.org/10.1021/acs.jpclett.2c03388
J. Phys. Chem. Lett. 2022, 13, 12049−12054

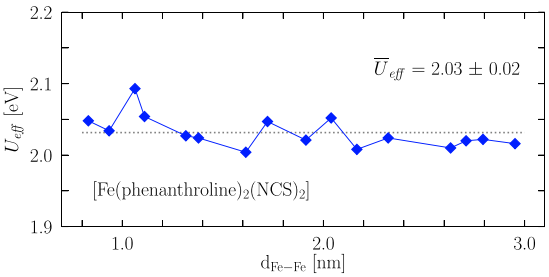

Figure 1. Comparison of the U_{eff} values, in units of eV, calculated with PBE at different Fe−Fe distances from a 6 × 6 × 6 supercell for the complex [Fe(phenanthroline)$_2$(NCS)$_2$]. The horizontal dotted line depicts the mean $\overline{U}_{eff}$ across all points and illustrates that the values of U_{eff} only depend weakly on the choice of structure.

- Identify the nearest-neighbor transition metal atom pair from the experimental unit cell. Isolate that pair of molecules in a sufficiently large computational unit cell.
- Optimize the geometry of the pair using the MS state with one molecule HS and the other LS.
- Determine U_{eff} for that MS pair using the linear response approach.[29]
- With U_{eff}, optimize the structures of both the pure LS and pure HS molecule pairs. Start both optimizations from the geometry found in the first step. Then calculate the adiabatic spin-crossover energy per molecule, also with U_{eff}, as $\Delta E_{HL} = (E_{HS_2} - E_{LS_2})/2$. The subscript 2 indicates total energy per pair.

A technical point is that the Hubbard correction includes the effective Coulomb and exchange interactions between parallel- and antiparallel-spin electrons, U and J, respectively. We adopted the common practice of incorporating J from parallel-spin electrons into an effective U as $U_{eff} = U - J$.[52]

All calculations were performed with periodic boundary conditions and the VASP code,[53] using the PBE approximation[54,55] for the XC functional. Details regarding the set of projector augmented wave potentials are included in Table S1 in the Supporting Information. The bimolecular species were placed inside orthorhombic boxes with at least 10 Å of vacuum separating the outermost atoms in every direction. The plane wave kinetic energy cutoff was set to 600 eV and the precision tolerance was set to "accurate". The augmentation charges were evaluated on an auxiliary support grid, aspheric corrections were included, and the use of symmetry was deactivated. The threshold for self-consistent field convergence was set to 10^{-6} eV, the Gaussian smearing width to 10^{-3} eV, and the projection operators were evaluated in reciprocal space. All geometries were optimized with the conjugate gradient algorithm until forces were smaller than 10^{-2} eV/Å.

To evaluate the mean-value ensemble method, we targeted a test set composed of spin-crossover metal−organic complexes that include the 3d transition metals Cr, Mn, Fe, Co, and Ni. This comprises the 20 complexes of ref 56 augmented by seven more,[57−65] as well as an additional subset of seven metal−organic complexes discarded in experimental screening tests.[63,66−71] The complete list is in the Supporting Information. Notice that we used [Fe((*N*-8-quino-lyl)-5-Br-salicylaldiminate)$_2$][NO$_3$] from ref 61 rather than [Fe(ethylenebis(acetylacetoneiminato))(NC$_5$H$_3$Me$_2$-3,4)$_2$] as in ref 56, due to difficulties in geometry relaxation associated with the large counterion used in the complex from the original test set.

Figure 2a compares the values of U_{eff} obtained using linear response on the MS state with those for the LS and HS states. The U_{eff} obtained for the LS and HS states are similar to one another and significantly larger than the values obtained for the MS state. Calculating U_{eff} using the MS state reduces the values by approximately a factor of 3 relative to results from the LS and HS states. We observe that different species sharing the same type of transition metal ion produce similar U_{eff}. In consequence, a smaller U_{eff} is expected to alleviate, at least partially, the overestimation of the total energy of the HS

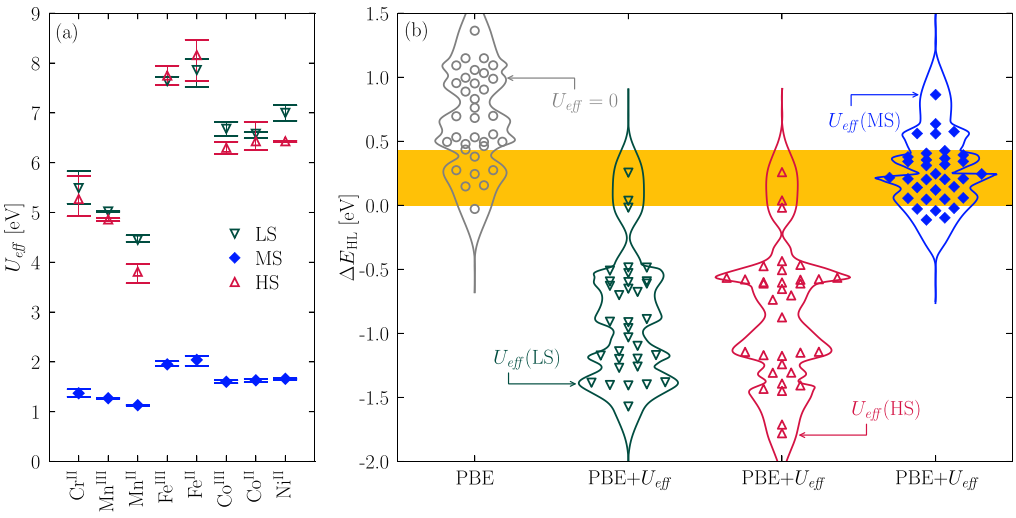

Figure 2. Results for the PBE and PBE+U_{eff} density functional approximations using the set of spin-crossover metal−organic complexes. (a) Comparison of the U_{eff} values, in eV, computed from linear response on the LS, HS, and MS states. The lower and upper limits depict the respective minimum and maximum U_{eff} obtained for each transition metal ion. (b) Adiabatic spin-crossover energy ΔE_{HL} distributions, in units of eV, for the whole set of metal−organic complexes. The shaded area encloses the energetic interval of interest for spin-crossover. The label $U_{eff} = 0$ depicts results with PBE, whereas the labels U_{eff}(LS), U_{eff}(HS), and U_{eff}(MS) depict results with PBE+U_{eff} using the U_{eff} value obtained from linear response on the LS, HS, and MS state, respectively.

https://doi.org/10.1021/acs.jpclett.2c03388
J. Phys. Chem. Lett. 2022, 13, 12049−12054

relative to the LS state, thereby yielding improved spin crossover energy predictions.

Next we compare the crossover energy differences, ΔE_{HL}, without and with the U_{eff} determined on the different spin states. Figure 2b shows how uncorrected PBE overestimates ΔE_{HL} with respect to the expected energy range. This behavior is well-documented.[72] The opposite behavior is observed for PBE+U_{eff} when the U_{eff} is obtained from either the LS or HS state. In those cases, most of the ΔE_{HL} are underestimated because of overcorrected HS total energies relative to the LS state. Use of the MS state gives a different trend. Unmistakably, the ΔE_{HL} values calculated with PBE+U_{eff} using the MS state are close to the expected energy range.[56,73] That is, the U_{eff} for this approximation leads to better balanced energy differences of the spin-states. The magnitude of this set of U_{eff} values is comparable to some reported in ref 74, though that work certainly is different for reasons of the systems considered there, the use of a different DFA, and because of various technical choices including cutoffs and choice of potentials. That said, what is rather suggestive for the spin-crossover problem is that they found somewhat smaller U_{eff} values than one ordinarily would expect.

Despite the well-known fact that U_{eff} is particular to each molecule or material, we observe similar values for each of the different transition metal ions across different molecular complexes in the data set (see Table S2 in the Supporting Information). Based on the observation that U_{eff} depends only mildly on the chemical environment of the transition metal ions, we recommend the averaged Hubbard-U_{eff} values, $\bar{U}_{eff}$, shown in Table 1, for PBE+U_{eff} calculations of spin crossover energies in automated high-throughput methods. The concept is to exploit the relatively low computational cost of PBE+U_{eff} as well as the betterment in the description of ΔE_{HL}. We emphasize that the addition of more molecular complexes to the test set will help refine these $\bar{U}_{eff}$ values.

Table 1. Averaged Effective Hubbard-U_{eff} Values, $\bar{U}_{eff}$, in Units of eV, for Common 3d Transition Metal Ions

	Cr^{II}	Mn^{III}	Mn^{II}	Fe^{III}	Fe^{II}	Co^{III}	Co^{II}	Ni^{II}
PBE	1.37	1.27	1.13	1.95	2.04	1.60	1.63	1.66

In conclusion, we showed that the mean-value spin ensemble provides an attractive reference state to obtain the value of the Hubbard-U_{eff} correction for accurate spin-crossover energy calculations with a simple DFA. Special ensembles have a long history of influence in DFT development and application. The scheme presented here involves methods of long-standing, namely broken-symmetry DFA+U calculations, in combination with a new type of special ensemble. We have shown that application to a mixed state typical of spin crossover enables successful use of linear response determination of Hubbard-U in calculations of ΔE_{HL} with a simple computationally low-cost DFA. Specifically, we have shown that the description of spin-crossover energies improves for PBE in combination with effective Hubbard-U_{eff} values calculated on a mean value ensemble state for a set of bistable metal−organic complexes. Based on the observed correlation between the calculated U_{eff} values and the oxidation state for each transition metal ion, we also provided a series of recommended averaged U_{eff} values for use in high-throughput calculations with PBE+U_{eff}. Finally, we note that there are diverse other molecular phenomena involving two or more spin states separated by comparatively small energy intervals,[75−81] which are computationally challenging. It remains to be tested whether the mean-value ensemble approach developed and tested can provide improvements regarding those phenomena comparable to the SCO improvements demonstrated here.

■ ASSOCIATED CONTENT

Supporting Information

The Supporting Information is available free of charge at https://pubs.acs.org/doi/10.1021/acs.jpclett.2c03388.

Optimized molecular geometries for the low- and high-spin states with the PBE and PBE+U_{eff} density functional approximations (TXT)

Data regarding the choice of projector augmented wave potentials in Table S1, Table S2 providing all the U_{eff} values for the metal−organic complexes and reference spin states, and Tables S3 and S4 further including results for frontier orbital energy differences and ΔE_{HL}, respectively, for all the molecular complexes (PDF)

■ AUTHOR INFORMATION

Corresponding Authors

S. B. Trickey − *Center for Molecular Magnetic Quantum Materials, Quantum Theory Project, University of Florida, Gainesville, Florida 32611, United States; Department of Physics and Department of Chemistry, University of Florida, Gainesville, Florida 32611, United States;* orcid.org/0000-0001-9224-6304; Email: trickey@ufl.edu

Richard G. Hennig − *Center for Molecular Magnetic Quantum Materials, Quantum Theory Project, University of Florida, Gainesville, Florida 32611, United States; Department of Materials Science and Engineering, University of Florida, Gainesville, Florida 32611, United States;* orcid.org/0000-0003-4933-7686; Email: rhennig@ufl.edu

Author

Angel Albavera-Mata − *Center for Molecular Magnetic Quantum Materials, Quantum Theory Project, University of Florida, Gainesville, Florida 32611, United States; Department of Materials Science and Engineering, University of Florida, Gainesville, Florida 32611, United States;* orcid.org/0000-0003-1521-678X

Complete contact information is available at: https://pubs.acs.org/10.1021/acs.jpclett.2c03388

Notes

The authors declare no competing financial interest.

■ ACKNOWLEDGMENTS

This work was supported as part of the Center for Molecular Magnetic Quantum Materials, an Energy Frontier Research Center funded by the U.S. Department of Energy, Office of Science, Basic Energy Sciences, under Award No. DE-SC0019330.

■ REFERENCES

(1) Gütlich, P.; Garcia, Y.; Goodwin, H. A. Spin crossover phenomena in Fe(II) complexes. *Chem. Soc. Rev.* **2000**, *29*, 419−427.

(2) Gütlich, P.; Goodwin, H. A.*Spin crossover in transition metal compounds*; Springer: Berlin and New York, 2004; pp 1−47.
(3) Bousseksou, A.; Molnár, G.; Salmon, L.; Nicolazzi, W. Molecular spin crossover phenomenon: Recent achievements and prospects. *Chem. Soc. Rev.* **2011**, *40*, 3313−3335.
(4) Gütlich, P.; Gaspar, A. B.; Garcia, Y. Spin state switching in iron coordination compounds. *Beilstein J. Org. Chem.* **2013**, *9*, 342−391.
(5) Janet, J. P.; Chan, L.; Kulik, H. J. Accelerating chemical discovery with machine learning: Simulated evolution of spin crossover complexes with an artificial neural network. *J. Phys. Chem. Lett.* **2018**, *9*, 1064−1071.
(6) Cuéllar, M. P.; Lapresta-Fernández, A.; Herrera, J. M.; Salinas-Castillo, A.; Pegalajar, M. d. C.; Titos-Padilla, S.; Colacio, E.; Capitán-Vallvey, L. F. Thermochromic sensor design based on Fe(II) spin crossover/polymers hybrid materials and artificial neural networks as a tool in modelling. *Sens. Actuators, B* **2015**, *208*, 180−187.
(7) Nandy, A.; Duan, C.; Janet, J. P.; Gugler, S.; Kulik, H. J. Strategies and software for machine learning accelerated discovery in transition metal chemistry. *Ind. Eng. Chem. Res.* **2018**, *57*, 13973−13986.
(8) Zhao, W.; Li, Q.; Huang, X.-H.; Bie, L.-H.; Gao, J. Toward the prediction of multi-spin state charges of a Heme model by random forest regression. *Front. Chem.* **2020**, *8*, 162.
(9) Nandy, A.; Duan, C.; Taylor, M. G.; Liu, F.; Steeves, A. H.; Kulik, H. J. Computational discovery of transition-metal complexes: From high-throughput screening to machine learning. *Chem. Rev.* **2021**, *121*, 9927−10000.
(10) Salomon, O.; Reiher, M.; Hess, B. A. Assertion and validation of the performance of the B3LYP* functional for the first transition metal row and the G2 test set. *J. Chem. Phys.* **2002**, *117*, 4729−4737.
(11) Paulsen, H.; Trautwein, A. K. Calculation of the electronic energy differences of spin crossover complexes. *J. Phys. Chem. Sol.* **2004**, *65*, 793−798.
(12) Lawson Daku, L. M.; Vargas, A.; Hauser, A.; Fouqueau, A.; Casida, M. E. Assessment of density functionals for the high-spin/low-spin energy difference in the low-spin iron(II) tris(2,2′-bipyridine) complex. *ChemPhysChem* **2005**, *6*, 1393−1410.
(13) Radoń, M. Revisiting the role of exact exchange in DFT spin-state energetics of transition metal complexes. *Phys. Chem. Chem. Phys.* **2014**, *16*, 14479−14488.
(14) Slimani, A.; Yu, X.; Muraoka, A.; Boukheddaden, K.; Yamashita, K. Reparametrization approach of DFT functionals based on the equilibrium temperature of spin-crossover compounds. *J. Phys. Chem. A* **2014**, *118*, 9005−9012.
(15) Harvey, J. N.*Principles and applications of density functional theory in inorganic chemistry I*; Springer Berlin Heidelberg: Berlin and Heidelberg, Germany, 2004; pp 151−184.
(16) Ganzenmüller, G.; Berkaïne, N.; Fouqueau, A.; Reiher, M.; Casida, M. E. Comparison of density functionals for differences between the high-($^5T_{2g}$) and low-($^1A_{1g}$) spin states of iron(II) compounds. IV. Results for the ferrous complexes [Fe(L)('NHS_4')]. *J. Chem. Phys.* **2005**, *122*, 234321.
(17) Ruzsinszky, A.; Perdew, J. P.; Csonka, G. I.; Vydrov, O. A.; Scuseria, G. E. Spurious fractional charge on dissociated atoms: Pervasive and resilient self-interaction error of common density functionals. *J. Chem. Phys.* **2006**, *125*, 194112.
(18) Ruzsinszky, A.; Perdew, J. P.; Csonka, G. I.; Vydrov, O. A.; Scuseria, G. E. Density functionals that are one- and two- are not always many-electron self-interaction-free, as shown for H_2^+, He_2^+, LiH^+, and Ne^+. *J. Chem. Phys.* **2007**, *126*, 104102.
(19) Cohen, A. J.; Mori-Sánchez, P.; Yang, W. Challenges for density functional theory. *Chem. Rev.* **2012**, *112*, 289−320.
(20) Perdew, J. P.; Parr, R. G.; Levy, M.; Baldúz, J. L., Jr. Density-functional theory for fractional particle number: Derivative discontinuities of the energy. *Phys. Rev. Lett.* **1982**, *49*, 1691−1694.
(21) Yang, X. D.; Patel, A. H. C.; Miranda-Quintana, R. A.; Heidar-Zadeh, F.; González-Espinoza, C. E.; Ayers, P. W. Two types of flat-planes conditions in density functional theory. *J. Chem. Phys.* **2016**, *145*, 031102.
(22) Hubbard, J. Electron correlations in narrow energy bands. *Proc. R. Soc. London A* **1963**, *276*, 238−257.
(23) Perdew, J. P.; Zunger, A. Self-interaction correction to density-functional approximations for many-electron systems. *Phys. Rev. B* **1981**, *23*, 5048−5079.
(24) Perdew, J. P.; Ruzsinszky, A.; Sun, J.; Pederson, M. E. Chapter one−paradox of self-interaction correction: How can anything so right be so wrong? *Adv. At. Mol. Opt. Phys.* **2015**, *64*, 1−14.
(25) Zope, R. R.; Yamamoto, Y.; Diaz, C. M.; Baruah, T.; Peralta, J. E.; Jackson, K. A.; Santra, B.; Perdew, J. P. A step in the direction of resolving the paradox of Perdew-Zunger self-interaction correction. *J. Chem. Phys.* **2019**, *151*, 214108.
(26) Anisimov, V. I.; Solovyev, I. V.; Korotin, M. A.; Czyżyk, M. T.; Sawatzky, G. A. Density-functional theory and NiO photoemission spectra. *Phys. Rev. B* **1993**, *48*, 16929−16934.
(27) Perdew, J. P.; Schmidt, K. Jacob's ladder of density functional approximations for the exchange-correlation energy. *AIP Conf. Proc.* **2001**, *577*, 1−20.
(28) Pickett, W. E.; Erwin, S. C.; Ethridge, E. C. Reformulation of the LDA+U method for a local-orbital basis. *Phys. Rev. B* **1998**, *58*, 1201−1209.
(29) Cococcioni, M.; de Gironcoli, S. Linear response approach to the calculation of the effective interaction parameters in the LDA+U method. *Phys. Rev. B* **2005**, *71*, 035105.
(30) Kulik, H. J.; Cococcioni, M.; Scherlis, D. A.; Marzari, N. Density functional theory in transition-metal chemistry: A self-consistent Hubbard *U* approach. *Phys. Rev. Lett.* **2006**, *97*, 103001.
(31) Himmetoglu, B.; Floris, A.; de Gironcoli, S.; Cococcioni, M. Hubbard-corrected DFT energy functionals: The LDA+U description of correlated systems. *Int. J. Quantum Chem.* **2014**, *114*, 14−49.
(32) Linscott, E. B.; Cole, D. J.; Payne, M. C.; O'Regan, D. D. Role of spin in the calculation of Hubbard *U* and Hund's *J* parameters from first principles. *Phys. Rev. B* **2018**, *98*, 235157.
(33) Perdew, J. P.; Levy, M. Physical content of the exact Kohn-Sham orbital energies: Band gaps and derivative discontinuities. *Phys. Rev. Lett.* **1983**, *51*, 1884−1887.
(34) Sham, L. J.; Schlüter, M. Density-functional theory of the energy gap. *Phys. Rev. Lett.* **1983**, *51*, 1888−1891.
(35) Tolba, S. A.; Gameel, K. M.; Ali, B. A.; Almossalami, H. A.; Allam, N. K.Chapter 1 The DFT+U: Approaches, accuracy, and applications. In *Density functional calculations*; Yang, G., Ed.; IntechOpen: Rijeka, Croatia, 2018; pp 3−30.
(36) Verma, P.; Truhlar, D. G. Does DFT+U mimic hybrid density functionals? *Theor. Chem. Acc.* **2016**, *135*, 182.
(37) Gani, T. Z. H.; Kulik, H. J. Where does the density localize? Convergent behavior for global hybrids, range separation, and DFT +U. *J. Chem. Theory Comput.* **2016**, *12*, 5931−5945.
(38) Pinter, B.; Chankisjijev, A.; Geerlings, P.; Harvey, J. N.; De Proft, F. Conceptual insights into DFT spin-state energetics of octahedral transition-metal complexes through a density difference analysis. *Chem. Eur. J.* **2018**, *24*, 5281−5292.
(39) Prokopiou, G.; Kronik, L. Spin-state energetics of Fe complexes from an optimally tuned range-separated hybrid functional. *Chem. Eur. J.* **2018**, *24*, 5173−5182.
(40) Mariano, L. A.; Vlaisavljevich, B.; Poloni, R. Biased spin-state energetics of Fe(II) molecular complexes within density-functional theory and the linear-response Hubbard *U* correction. *J. Chem. Theory Comput.* **2020**, *16*, 6755−6762.
(41) Mariano, L.; Vlaisavljevich, B.; Poloni, R. Improved spin-state energy differences of Fe(II) molecular and crystalline complexes via the Hubbard U-corrected density. *J. Chem. Theory Comput.* **2021**, *17*, 2807−2816.
(42) Lebègue, S.; Pillet, S.; Ángyán, J. G. Modeling spin-crossover compounds by periodic DFT+U approach. *Phys. Rev. B* **2008**, *78*, 024433.
(43) Panchmatia, P. M.; Ali, M. E.; Sanyal, B.; Oppeneer, P. M. Halide ligated iron porphines: A DFT+U and UB3LYP study. *J. Phys. Chem. A* **2010**, *114*, 13381−13387.

https://doi.org/10.1021/acs.jpclett.2c03388
J. Phys. Chem. Lett. 2022, 13, 12049−12054

(44) Maldonado, P.; Kanungo, S.; Saha-Dasgupta, T.; Oppeneer, P. M. Two-step spin-switchable tetranuclear Fe(II) molecular solid: *ab initio* theory and predictions. *Phys. Rev. B* **2013**, *88*, 020408.
(45) Vela, S.; Fumanal, M.; Cirera, J.; Ribas-Arino, J. Thermal spin crossover in Fe(II) and Fe(III). Accurate spin state energetics at the solid state. *Phys. Chem. Chem. Phys.* **2020**, *22*, 4938−4945.
(46) Mejía-Rodríguez, D.; Albavera-Mata, A.; Fonseca, E.; Chen, D.-T.; Cheng, H.-P.; Hennig, R. G.; Trickey, S. B. Barriers to predictive high-throughput screening for spin-crossover. *Comput. Mater. Sci.* **2022**, *206*, 111161.
(47) Slater, J. C. In *Computational methods in band theory*; Marcus, P., Janak, J. F., Williams, A. R., Eds.; Plenum Press: New York, 1971; p 447.
(48) Trickey, S. B. Ensemble-representable reduced density matrices suggested by the Xα transition state. *Chem. Phys. Lett.* **1973**, *21*, 581−585.
(49) Köhler, C. P.; Jakobi, R.; Meissner, E.; Wiehl, L.; Spiering, H.; Gütlich, P. Nature of the phase transition in spin crossover compounds. *J. Phys. Chem. Solids* **1990**, *51*, 239−247.
(50) Klingele, M. H.; Moubaraki, B.; Cashion, J. D.; Murray, K. S.; Brooker, S. The first x-ray crystal structure determination of a dinuclear complex trapped in the [low spin−high spin] state: $[Fe_2^{ii}(PMAT)_2](BF_2)_4$·DMF. *Chem. Commun.* **2005**, *2005*, 987−989.
(51) Timrov, I.; Marzari, N.; Cococcioni, M. Self-consistent Hubbard parameters from density-functional perturbation theory in the ultrasoft and projector-augmented wave formulations. *Phys. Rev. B* **2021**, *103*, 045141.
(52) Dudarev, S. L.; Botton, G. A.; Savrasov, S. Y.; Humphreys, C. J.; Sutton, A. P. Electron-energy-loss spectra and the structural stability of nickel oxide: An LSDA+U study. *Phys. Rev. B* **1998**, *57*, 1505−1509.
(53) Kresse, G.; Furthmüller, J. Efficient iterative schemes for *ab initio* total-energy calculations using a plane-wave basis set. *Phys. Rev. B* **1996**, *54*, 11169−11186.
(54) Perdew, J. P.; Burke, K.; Ernzerhof, M. Generalized gradient approximation made simple. *Phys. Rev. Lett.* **1996**, *77*, 3865−3868.
(55) Perdew, J. P.; Burke, K.; Ernzerhof, M. Errata: Generalized gradient approximation made simple. *Phys. Rev. Lett.* **1997**, *78*, 1396.
(56) Cirera, J.; Via-Nadal, M.; Ruiz, E. Benchmarking density functional methods for calculation of state energies of first row spin-crossover molecules. *Inorg. Chem.* **2018**, *57*, 14097−14105.
(57) Sitzmann, H.; Schar, M.; Dormann, E.; Kelemen, M. Octaisopropylchromocen: Das erste chromocen mit kontinuierlichem low spin/high spin-übergang. *Z. anorg. allg. Chem.* **1997**, *623*, 1850−1852.
(58) Shay, D. T.; Yap, G. P. A.; Zakharov, L. N.; Rheingold, A. L.; Theopold, K. H. Intramolecular C−H activation by an open-shell cobalt(III) imido complex. *Angew. Chem., Int. Ed.* **2005**, *44*, 1508−1510.
(59) Shay, D. T.; Yap, G. P. A.; Zakharov, L. N.; Rheingold, A. L.; Theopold, K. H. Corrigendum: Intramolecular C−H activation by an open-shell cobalt(III) imido complex. *Angew. Chem., Int. Ed.* **2006**, *45*, 7870.
(60) King, E. R.; Sazama, G. T.; Betley, T. A. Co(III) imidos exhibiting spin crossover and C−H bond activation. *J. Am. Chem. Soc.* **2012**, *134*, 17858−17861.
(61) Harding, D. J.; Phonsri, W.; Harding, P.; Murray, K. S.; Moubaraki, B.; Jameson, G. N. L. Abrupt two-step and symmetry breaking spin crossover in an iron(III) complex: An exceptionally wide [ls−hs] plateau. *Dalton Trans* **2015**, *44*, 15079−15082.
(62) Homma, Y.; Ishida, T. A new $S = 0 \rightleftarrows S = 2$ "spin-crossover" scenario found in a nickel(II) bis(nitroxide) system. *Chem. Matter.* **2018**, *30*, 1835−1838.
(63) Kyoden, Y.; Homma, Y.; Ishida, T. High-spin and incomplete spin-crossover polymorphs in doubly chelated $[Ni(L)_2Br_2]$ (L = *tert*-butyl 5-phenyl-2-pyridyl nitroxide). *Inorg. Chem.* **2019**, *58*, 10743−10755.
(64) Becker, P. M.; Förster, C.; Carrella, L. M.; Boden, P.; Hunger, D.; van Slageren, J.; Gerhards, M.; Rentschler, E.; Heinze, K. Spin crossover and long-lived excited states in a reduced molecular ruby. *Chem. Eur. J.* **2020**, *26*, 7199−7204.
(65) Gakiya-Teruya, M.; Jiang, X.; Le, D.; Üngör, Ö.; Durrani, A. J.; Koptur-Palenchar, J. J.; Jiang, J.; Jiang, T.; Meisel, M. W.; Cheng, H.-P.; et al. Asymmetric design of spin-crossover complexes to increase the volatility for surface deposition. *J. Am. Chem. Soc.* **2021**, *143*, 14563−14572.
(66) Guionneau, P.; Marchivie, M.; Bravic, G.; Létard, J.-F.; Chasseau, D. Co(II) molecular complexes as a reference for the spin crossover in Fe(II) analogues. *J. Mater. Chem.* **2002**, *12*, 2546−2551.
(67) Meredith, M. B.; Crisp, J. A.; Brady, E. D.; Hanusa, T. P.; Yee, G. T.; Brooks, N. R.; Kucera, B. E.; Young, V. G. High-spin and spin-crossover behavior in monomethylated bis(indenyl)chromium(II) complexes. *Organometallics* **2006**, *25*, 4945−4952.
(68) Sertphon, D.; Harding, D. J.; Harding, P.; Murray, K. S.; Moubaraki, B.; Cashion, J. D.; Adams, H. Anionic tuning of spin crossover in Fe^{III}-quinolylsalicylaldiminate complexes. *Eur. J. Inorg. Chem.* **2013**, *2013*, 788−795.
(69) Luo, Y.-H.; Wen, G.-J.; Gu, L.-S.; Wang, M.-N.; Sun, B.-W. Study of spin crossover in an iron(II) tris(diimine) system tuned by counter anions. *Polyhedron* **2017**, *121*, 101−106.
(70) Piskunov, A. V.; Pashanova, K. I.; Ershova, I. V.; Bogomyakov, A. S.; Smolyaninov, I. V.; Starikov, A. G.; Kubrin, S. P.; Fukin, G. K. Pentacoordinated cloro-bis-*o*-iminosemiquinonato Mn^{III} and Fe^{III} complexes. *J. Mol. Struct.* **2018**, *1165*, 51−61.
(71) Wang, H.; Baldé, C.; Grosjean, A.; Desplanches, C.; Guionneau, P.; Chastanet, G. Seven-coordinated iron(II) spin-crossover molecules: Some learning from iron substitution in $[Fe_xMn_{1-x}(L_{222}N_3O_2)(CN)_2]$·$H_2O$ solid solutions. *Dalton Trans* **2018**, *47*, 14741−14750.
(72) Kepp, K. P. Theoretical study of spin crossover in 30 iron complexes. *Inorg. Chem.* **2016**, *55*, 2717−2727.
(73) Kepp, K. P. In *Transition metals in coordination environments. Challenges and advances in computational chemistry and physics*; Broclawik, E., Borowski, T., Radoń, M., Eds.; Springer International Publishing: Cham, Switzerland, 2019; pp 1−33.
(74) Sai Gautam, G.; Carter, E. A. Evaluating transition metal oxides within DFT-SCAN and SCAN+*U* frameworks for solar thermochemical applications. *Phys. Rev. Mater.* **2018**, *2*, 095401.
(75) Ghosh, A. Transition metal spin state energetics and noninnocent systems: Challenges for DFT in the bioinorganic arena. *J. Biol. Inorg. Chem.* **2006**, *11*, 712−724.
(76) Miller, J. S.; Min, K. S. Oxidation leading to reduction: Redox-induced electron transfer (RIET). *Angew. Chem., Int. Ed.* **2009**, *48*, 262−272.
(77) Chirik, P. J.; Wieghardt, K. Radical ligands confer nobility on base-metal catalysts. *Science* **2010**, *327*, 794−795.
(78) Kaim, W. Manifestations of noninnocent ligand behavior. *Inorg. Chem.* **2011**, *50*, 9752−9765.
(79) Praneeth, V. K. K.; Ringenberg, M. R.; Ward, T. R. Redox-active ligands in catalysis. *Angew. Chem., Int. Ed.* **2012**, *51*, 10228−10234.
(80) Chirik, P.; Morris, R. Getting down to Earth: The renaissance of catalysis with abundant metals. *Acc. Chem. Res.* **2015**, *48*, 2495−2495.
(81) Echegaray, E.; Toro-Labbe, A.; Dikmenli, K.; Heidar-Zadeh, F.; Rabi, N.; Rabi, S.; Ayers, P. W.; Cardenas, C.; Parr, R. G.; Anderson, J. S. M. In *Correlations in Condensed Matter under Extreme Conditions: A tribute to Renato Pucci on the occasion of his 70th birthday*; Angilella, G. G. N., Ed.; Springer International Publishing: Cham, Switzerland, 2017; pp 269−278.

https://doi.org/10.1021/acs.jpclett.2c03388
J. Phys. Chem. Lett. 2022, 13, 12049−12054